Anisotropic Interactions of Hydrogen Molecules from the Pressure Dependence of the Rotational Spectrum in the $Ar(H_2)_2$ Compound

Francesco Grazzi,[1,3,4,*] Mario Santoro,[3,4,†] Massimo Moraldi,[1,3,‡] and Lorenzo Ulivi[2,3,4,§]

[1]*Dipartimento di Fisica dell'Università, largo Enrico Fermi 2, I-50125 Firenze, Italy*
[2]*Istituto di Elettronica Quantistica, CNR, via Panciatichi 56/30 , I-50127 Firenze, Italy*
[3]*Istituto Nazionale di Fisica della Materia (INFM) Unità di Firenze, largo Enrico Fermi 2, I-50125 Firenze, Italy*
[4]*Laboratorio Europeo di Spettroscopie Non Lineari (LENS), largo Enrico Fermi 2, I-50125 Firenze, Italy*

(Received 11 May 2001; published 4 September 2001)

We report the pressure evolution, up to 70 GPa, of the fine structure of the $S_0(0)$ rotational excitation in the high-pressure $Ar(H_2)_2$ compound (with almost 100% para-H_2) at about 30 K. A perturbative theoretical analysis is developed to calculate intensities and frequency shifts of the active Raman rotational components, on the basis of the intermolecular anisotropic interaction. The comparison between experimental results up to 35 GPa and calculation allows a reliable determination of the anisotropic intermolecular potential in the solid, both for H_2—H_2 and H_2—Ar at short range. Such results are important for the interpretation of the high-pressure orientational properties of solid hydrogen.

DOI: 10.1103/PhysRevLett.87.125506 PACS numbers: 62.50.+p, 34.20.Gj, 78.30.–j

The high-pressure properties of the solid hydrogens are far from being clarified and continue to attract great interest [1,2]. Solid hydrogen molecules are weakly interacting and stable up to the megabar range. Their quantum rotational states differ only slightly from the free-rotor states, up to relatively high pressure. A description in terms of an intermolecular interaction potential is then particularly meaningful, and allows the calculation, from first principle quantum theory, of many spectroscopic properties [3]. Several models for the isotropic potential exist, some of which are derived from molecular beam cross section and gas phase properties, some from *ab initio* computations on isolated pairs [4–7], and some others from the solid equation of state [8]. Anisotropic interaction components have also been derived; however, these are less reliable, especially at short intermolecular distances. The transition to the rotationally ordered high-pressure phases of H_2 and the structure of these phases can possibly be described by an accurate knowledge of this anisotropic interaction. Therefore it is quite useful to study the spectrum of the rotational excitations (rotons) that is determined by these anisotropic interactions.

In pure solid parahydrogen, the splitting of the $S_0(0)$ Raman line into a triplet has demonstrated the hexagonal close packed (hcp) structure of the low pressure solid [3] and its disappearance with rising pressure has revealed the transition to the ordered phase [9,10]. The analysis of this splitting has been done in the past considering only the strongest electric quadrupole-quadrupole (EQQ) interaction [11]. The effect of the other components is usually neglected, because of the symmetry of the hcp lattice. However, in a recent study up to 70 GPa [12] the authors propose that other components of the anisotropic H_2—H_2 interactions, different from the EQQ, may play a significant role.

In this paper we demonstrate that anisotropic components of the H_2—H_2 interaction can be measured with great sensitivity from the analysis of the pure rotational Raman band $S_0(0)$, in the stoichiometric compound $Ar(H_2)_2$. The theoretical analysis of the rotational bands in $Ar(H_2)_2$, on the basis of perturbation theory, is also developed in this paper. This permits one to calculate the frequency positions, intensities, and symmetry properties of the $S_0(0)$ components, on the basis of the anisotropic H_2—H_2 and H_2—Ar interaction potentials. On the other hand, measurements of the polarization properties of the band components permit one to assign the experimental frequencies to the theoretical ones. It is of importance that, in contrast to the case of pure H_2, in $Ar(H_2)_2$ crystal field effects do not cancel out, allowing the possibility to measure components of the anisotropic potential with symmetry different from the one of the EQQ term.

The $Ar(H_2)_2$ crystal has been prepared at room temperature, the pressure slowly rising above solidification (4.3 GPa) of an Ar/H_2 gas mixture in stoichiometric proportion inside a diamond anvil cell (DAC). The crystal space group, known from synchrotron x-ray diffraction [13], is D_{6h}^4 ($P6_3/mmc$) with eight H_2 molecules and four Ar atoms in the unit cell. All the samples are single crystals with the crystallographic c axis along the cell axis. This is shown by the presence of a faceted (hexagonal) crystal during the growth process. In $Ar(H_2)_2$, as in solid H_2, the molecules rotate almost freely, and their vibrational interaction is described quantitatively in both solids by the same model [14]. Details of the forward-scattering Raman setup are described in Ref. [15]. Pure para-H_2 is obtained by taking advantage of the increased intrinsic conversion rate in a solid sample of $Ar(H_2)_2$ at high pressure [15], which is of the same order of magnitude as the one measured in solid H_2 [16]. When conversion is almost complete ($\simeq 3\%$ ortho-H_2), the $S_0(0)$ band develops a fine structure, showing several peaks that, at a pressure of 6 GPa, spread over a frequency range of about 100 cm^{-1} (see Fig. 1).

We performed several isothermal scans at about 30 K up to a maximum pressure of 68 GPa. Pressure in the sample has been determined by the ruby scale [17]. The values of the line positions, intensities, and widths have been derived for every pressure. The peaks, whose frequency rises with pressure with a much higher slope than the average one, are assigned to lattice phonon excitations.

Polarization analysis has been of fundamental help to identify the various components of the band, and to compare with theory. This has been possible because the orientation of the crystal is known, overcoming the serious experimental difficulties, due to the depolarization of the radiation by the two stressed diamonds, with the combined use of a Babinet-Soleil compensator and of a polarizer after the DAC [18]. In Fig. 2 we report two spectra measured at 14.9 GPa in the VH and the VV configurations, where the first V indicates vertical incident polarization on the sample, and the second letter the analyzed component of the scattered radiation. It is evident that the two intense lines at 353 and 391 cm^{-1} and the weak one at 454 cm^{-1} are polarized, while the others are nonpolarized. The extinction ratio appears lower for the 353 cm^{-1} line, probably because other nonpolarized components give some contribution close to this frequency.

We use quantum mechanical perturbation theory to evaluate the energies of the rotational $S_0(0)$ states, similar to the method described for solid H_2 [19], assuming rigid H_2 molecules on a rigid lattice. The anisotropic interaction energy is small with respect to the rotational energy, and it is taken into account in a first order perturbative treatment. It removes the m degeneracy and couples the components of the rotational excitations of different molecules, but does not mix states with different J's. The wave function for the $J = 2$, $\mathbf{k} = 0$, rotational excitations is written as a linear combination of spherical harmonics of the orientations Ω_{qp} of the pth molecule in the qth unit cell, that is,

$$\psi = \sum_q \sum_{p=1}^{8} \sum_{m=-2}^{+2} C_{pm} Y_{2m}(\Omega_{qp}) . \qquad (1)$$

There are forty linearly independent ψ functions due to the eight H_2 molecules present in the cell and to the five possible m values. Because of the symmetry properties of the anisotropic part of the polarizability in the D_{6h} rotation group of the crystal [20], only three wave functions of symmetry A_{1g}, four of symmetry E_{1g}, and five of symmetry E_{2g} can give rise to Raman transitions from the ground state. In order to calculate the frequencies and the intensities of the active modes, it is necessary to write down explicitly basis functions for these irreducible representations that are not reported here. We assume that the crystal polarizability is composed only of single molecule contributions and the potential energy is pairwise additive. In this case it turns out that only three E_{1g} and four E_{2g} lines are Raman allowed [18] so that only ten lines are to be expected.

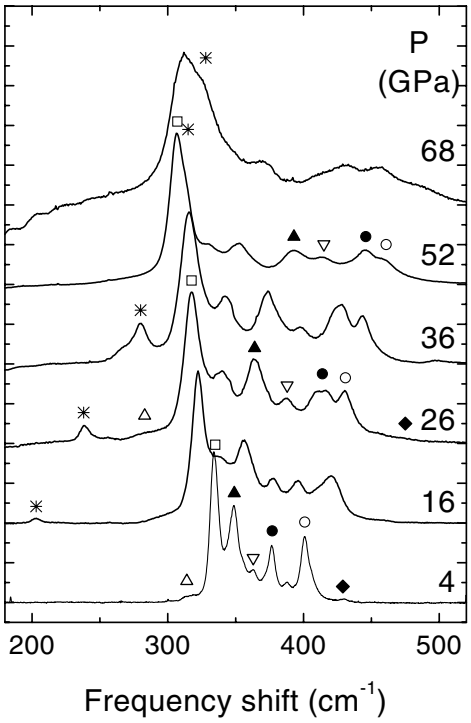

FIG. 1. Experimental Raman spectra of the $S_0(0)$ band at different pressures. Full and empty symbols mark some polarized and nonpolarized rotational components, respectively, and $*$ marks one band assigned to a lattice phonon.

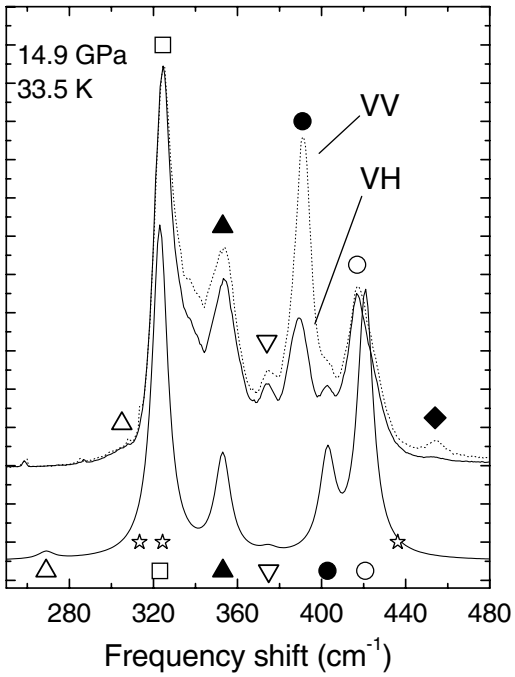

FIG. 2. Upper lines: experimental spectra obtained with different polarization at a pressure of 14.9 GPa. Bottom line: Spectrum calculated at the same pressure, attributing to each component a Lorentzian shape. Full symbols, empty symbols, and stars mark A_{1g}, E_{2g}, E_{1g} $S_0(0)$ components, respectively. Upper symbols refer to experimental data as in Fig. 1, and bottom symbols refer to calculated components.

The radiation collected in our scattering geometry is due to the components α_{xx} and α_{xy} of the polarizability that transform as A_{1g} and E_{2g}. Therefore the lines associated with the E_{1g} states are either absent or very weak in the experimental spectrum.

The anisotropic potential energy V is given by the sum of the $v^{(H_2-H_2)}$ and $v^{(H_2-Ar)}$ pair interactions. The pair intermolecular potential functions v are expanded in spherical components as in Ref. [21].

For H_2—Ar pairs, the literature models for the anisotropic interaction energy v^{H_2-Ar} [22,23] are limited to the spherical component V_{202}. For H_2—H_2 various semiempirical analytic expressions have been derived based on experimental data [5,6], or on *ab initio* computation [7]. We will consider the components $V_{202} = V_{022}$, responsible for crystal field effects, and V_{224}, which give rise to propagating rotonic excitations. Other components (V_{222}) which may give a splitting are discussed later. No reliable information exists in the literature about V_{404} for both H_2—H_2 and H_2—Ar.

To represent the R dependence of the V_{202} potential components we use analytic functions of the form [5,22]

$$V_{202}(R) = A\exp(-\beta R) - D(R)\left[\frac{C_6}{R^6} + \frac{C_8}{R^8} + \frac{C_{10}}{R^{10}}\right], \tag{2}$$

where $D(R) = \exp[-a(R_0/R - 1)^c]$ for $R \le R_0$ and $D(R) = 1$ for $R \ge R_0$ with (a, c) integer numbers. Values for the parameters are listed in Table I both for H_2—Ar and H_2—H_2.

The numerical calculation of Raman line positions and intensities reduces to suitable lattice sums of the potential components [18]. The density, and thus the intermolecular distance, has been derived using the $Ar(H_2)_2$ equation of state determined by x-ray diffraction [24].

With the anisotropic interaction potential components reported in Refs. [5–7,22,23], the agreement with the experiment is not satisfactory, resulting, on the average, in a too small separation of the lines at low pressure, compared with the experimental one. The comparison is shown in Fig. 3(a) as a function of pressure, where the full and dashed lines represent A_{1g} and E_{2g} components, respectively. For this comparison, a constant shift has been applied to the theoretical frequencies, forcing the agreement for the most intense component (empty squares).

We show that it is justified to attribute such a discrepancy to the inaccuracy of the potential models. In the case of H_2—Ar, for example, the interaction potential is reliable only for $R \ge 3.2$ Å [22], while the nearest-neighbor (nn) H_2—Ar distances relevant for this experiment are in the range 2.2–2.7 Å. We have then used our data to model the potential components V_{202}, V_{224} (H_2—H_2), and V_{202} (H_2—Ar), mainly changing the repulsive hard core, to obtain a better fit of the experimental spectrum. To judge the accuracy of the fit not only the frequency positions but also the intensities have been considered. Large changes in the rotational frequencies are obtained even for a very small change in the potential model, revealing the sensitivity of the spectrum to the fine details of the anisotropic interaction. The comparison is shown in Fig. 3(b), and it is satisfactory for most of the components. The largest discrepancies are observed for the two extreme lines that, however, are very weak. At pressure above 30–40 GPa we believe that the first order perturbative approach may not be sufficient, and we do not consider relevant the disagreement observed. For completeness, we report in Fig. 2 also

TABLE I. Parameters of the anisotropic V_{202} components of the H_2—Ar and H_2—H_2 potentials. Units are cm^{-1} for energies and Å lengths.

	H_2—Ar This work	H_2—H_2 Ref. [5]	H_2—H_2 Ref. [7]	H_2—H_2 This work
A	7.579×10^5	2.881×10^4	3.615×10^4	1.523×10^5
β	3.45	3.02	2.9	3.4
C_6	2700	1224	1224	1224
C_8	78 000	16 400	16 400	16 400
C_{10}	0	114 000	487 000	232 000
a	4	1	1	1
c	3	2	2	2
R_0	3.5727	5.82	5.82	5.82
R_e	3.82	3.627	3.583	3.72
ϵ	1.16	0.459	0.636	0.505

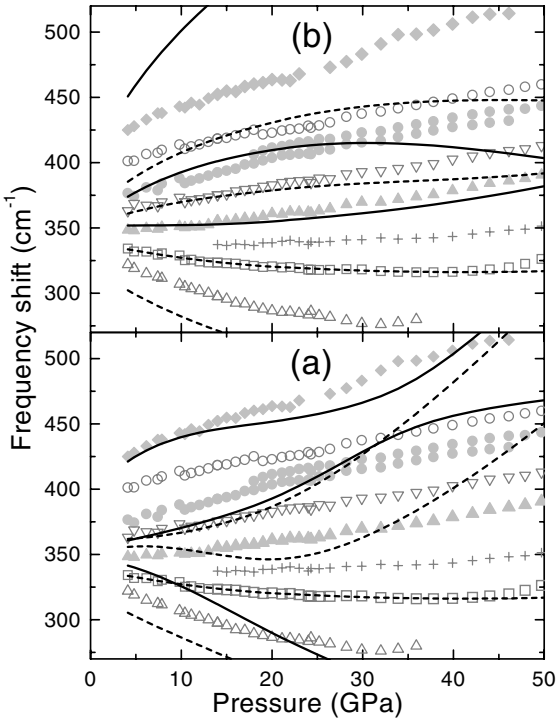

FIG. 3. Comparison of the experimental frequency positions (symbols as in Fig. 2) with the calculation (full lines, A_{1g} components; dashed lines, E_{2g} components) using either the anisotropic potential models quoted in the literature (a) or the modified ones (b) as described in the text.

the theoretical spectrum obtained attributing to each component a Lorentzian shape with the same width, similar to the measured ones. Our results for the V_{224} component for H_2—H_2 essentially coincides with those of Ref. [6]. In Table I we report the values of the parameters of the V_{202} potential models [Eq. (2)] obtained by our fit, with those of Ref. [5] and those that reproduce the numerical results of Ref. [7]. The V_{202} component for H_2—Ar obtained by the fit agrees with previously reported results within a 10% discrepancy. On the other hand, much larger differences are seen for the V_{202} component for H_2—H_2, which is almost twice as large as the result of Refs. [5,6] at short distance, the difference amounting to about $15-20\ \mathrm{cm}^{-1}$ at 2.2 Å. The difference with the *ab initio* results of Ref. [7] is slightly smaller.

To assess the reliability of our determination, the effect of the small component of the type 222 of the H_2—H_2 potential [6] has also been taken into account. The inclusion of such a contribution changes the rotational energy shifts by less than 3% and does not appreciably change the fitted potential parameters. The effects related to the zero point motion of the centers of mass of the molecules, which are neglected in the rigid lattice approach, are probably of the same order of magnitude (about 5% at the densities of our interest) of those calculated for the EQQ interaction [25]. On the other hand, the anisotropic interaction derived from molecular beam cross sections and gas phase data is influenced by the problem that the dynamics of rotations is strongly affected by the isotropic part of the potential which determines the trajectories of the molecules. Therefore a small variation in the assumed isotropic part of the potential is reflected in a relatively larger variation in the anisotropic components. Such a drawback is absent in our method because the isotropic potential affects the orientational dynamics only through the small zero point motion.

Finally, we can notice that many body effects could affect our results. Unfortunately, little is known about three-body contributions to the intermolecular potential and it refers only to long range dispersion terms [26]. Moreover, a theory for the inclusion of three-body potentials in the calculation of rotational energy is still lacking. Our potential can indeed contain effectively many body terms being in any case of practical use for the application to solid state properties, as has been done for the isotropic potential. We therefore believe that the results obtained in this work may be extremely valuable, due to the high (and highly selective) sensitivity, for calculations concerned with high-pressure properties of solid hydrogen, specifically the structure of the ordered phases.

Useful discussions with F. Barocchi are gratefully acknowledged. This work has been supported by the European Union, under Contract No. HPRICT1999-00111.

*Electronic address: grazzi@fi.infn.it
†Electronic address: santoro@lens.unifi.it
‡Electronic address: moraldi@fi.infn.it
§Electronic address: ulivi@ieq.fi.cnr.it

[1] I. F. Silvera, Rev. Mod. Phys. **52**, 393 (1980).
[2] H. K. Mao and R. J. Hemley, Rev. Mod. Phys. **66**, 671 (1994).
[3] J. Van Kranendonk, *Solid Hydrogen* (Plenum Press, New York, 1983).
[4] G. T. McConville, J. Chem. Phys. **74**, 2201 (1981).
[5] M. J. Norman, R. O. Watts, and U. Buck, J. Chem. Phys. **81**, 3500 (1984).
[6] J. Schaefer and W. E. Koehler, Z. Phys. D **13**, 217 (1989).
[7] P. Diep and J. K. Johnson, J. Chem. Phys. **112**, 4465 (2000).
[8] I. F. Silvera and W. W. Goldman, J. Chem. Phys. **69**, 4209 (1978).
[9] H. E. Lorenzana, I. F. Silvera, and K. A. Goettel, Phys. Rev. Lett. **64**, 1939 (1990).
[10] I. F. Silvera and R. J. Wijngaarden, Phys. Rev. Lett. **47**, 39 (1981).
[11] P. Loubeyre, M. Jean-Louis, and I. F. Silvera, Phys. Rev. B **43**, 10 191 (1991).
[12] A. F. Goncharov, M. A. Strzhemechny, H. K. Mao, and R. J. Hemley, Phys. Rev. B **63**, 064304 (2001).
[13] P. Loubeyre, R. LeToullec, and J.-P. Pinceaux, Phys. Rev. Lett. **72**, 1360 (1994).
[14] L. Ulivi, R. Bini, P. Loubeyre, R. LeToullec, and H. J. Jodl, Phys. Rev. B **60**, 6502 (1999).
[15] F. Grazzi and L. Ulivi, Europhys. Lett. **52**, 564 (2000).
[16] J. H. Eggert, E. Karmon, R. J. Hemley, H. K. Mao, and A. F. Goncharov, Proc. Natl. Acad. Sci. U.S.A. **96**, 12 269 (1999).
[17] H. K. Mao, P. M. Bell, J. V. Shaner, and D. J. Steinberg, J. Appl. Phys. **49**, 3276 (1978).
[18] F. Grazzi, M. Santoro, M. Moraldi, and L. Ulivi (to be published).
[19] See paragraph 4.2.2. of Ref. [3].
[20] L. Landau and E. Lifchitz, *Mécanique Quantique* (Mir Editions, Moscow, 1974).
[21] J. Schaefer and W. Meyer, J. Chem. Phys. **70**, 344 (1979).
[22] R. J. Le Roy and J. S. Carley, Adv. Chem. Phys. **42**, 353 (1980).
[23] R. J. Le Roy and J. M. Hutson, J. Chem. Phys. **86**, 837 (1987).
[24] P. Loubeyre (private communication).
[25] V. V. Goldman, Phys. Rev. B **20**, 4478 (1979).
[26] S. A. C. McDowell and W. J. Meath, Mol. Phys. **90**, 713 (1997).